Chapter 22

Why cycle?

> "Progress was a labyrinth ... people plunging blindly in and then rushing wildly back, shouting that they had found it ... the invisible king - the élan vital - the principle of evolution ... writing a book, starting a war, founding a school...."
>
> —F. Scott Fitzgerald, *This Side of Paradise*

In the preceding chapters we have moved rather briskly through the evolution operator formalism. Here we slow down in order to develop some fingertip feeling for the traces of evolution operators. It is a melancholy task, as the "intuition" garnered by these heuristic approximations is in all ways inferior to the straightforward and exact theory developed so far. But, it has to be done, as there is immense literature out there that deploys these heuristic estimates, most of it of it uninspired, some of it plain wrong, and the reader should be able to understand and sort through that literature. We start out by explaining qualitatively how local exponential instability of topologically distinct trajectories leads to a global exponential instability.

22.1 Escape rates

We start by verifying the claim (17.11) that for a nice hyperbolic flow the trace of the evolution operator grows exponentially with time. Consider again the game of pinball in figure 1.1. Designate by $\mathcal{M}$ a region of state space that encloses the three disks, such as the surface of the table along with all pinball directions. The fraction of initial points whose trajectories start within $\mathcal{M}$ and recur within that region at the time t is given by

$$\hat{\Gamma}_{\mathcal{M}}(t) = \frac{1}{|\mathcal{M}|}\int\int_{\mathcal{M}} dxdy\,\delta\big(y - f^t(x)\big)\,. \tag{22.1}$$

This quantity is both measurable and physically interesting in a variety of problems spanning nuclear physics to celestial mechanics. The integral over x takes care of all possible initial pinballs; the integral over y checks whether they are still within $\mathcal{M}$ by time t. If the dynamics is bounded, and $\mathcal{M}$ envelops the entire accessible state space, $\hat{\Gamma}_{\mathcal{M}}(t) = 1$ for all t. However, if trajectories exit $\mathcal{M}$, the recurrence fraction decreases with time. For example, any trajectory that falls off the pinball table in figure 1.1 is gone for good.

These observations can be made more concrete by examining the pinball phase-space of figure 1.9. With each pinball bounce the initial conditions that survive get thinned out, each strip yielding two thinner strips within it. The total fraction of survivors (1.2) after n bounces is given by

$$\hat{\Gamma}_n = \frac{1}{|\mathcal{M}|}\sum_i^{(n)} |\mathcal{M}_i|\,, \tag{22.2}$$

where i is a binary label of the ith strip, and $|\mathcal{M}_i|$ is the area of the ith strip. Phase-space volume is preserved by the flow, so the strips of survivors are contracted along the stable eigen-directions and ejected along the unstable eigen-directions. As a crude estimate of the number of survivors in the ith strip, assume that a ray of trajectories spreads by a factor Λ after every bounce. The quantity Λ represents the mean value of the expanding eigenvalue of the corresponding Jacobian matrix of the flow. We replace $|\mathcal{M}_i|$ by the phase-space strip width estimate $|\mathcal{M}_i|/|\mathcal{M}| \sim 1/\Lambda_i$, which is right in spirit but not without drawbacks. For example, in general the eigenvalues of a Jacobian matrix for a finite segment of a trajectory have no invariant meaning; they depend on the choice of coordinates. However, we saw in chapter 18 that neighborhood sizes are determined by Floquet multipliers of periodic points, which are invariant under smooth coordinate transformations.

In the approximation $\hat{\Gamma}_n$ receives 2^n contributions of equal size

$$\hat{\Gamma}_1 \sim \frac{1}{\Lambda} + \frac{1}{\Lambda}, \cdots \qquad , \hat{\Gamma}_n \sim \frac{2^n}{\Lambda^n} = e^{-n(\lambda - h)} = e^{-n\gamma}\,, \tag{22.3}$$

up to pre-exponential factors. We see here the interplay of the two key ingredients of chaos first mentioned in sect. 1.3.1: the escape rate γ equals the local expansion rate (the Lyapunov exponent $\lambda = \ln\Lambda$) minus the rate of global reinjection back into the system (the topological entropy $h = \ln 2$).

At each bounce one routinely loses the same fraction of trajectories, so one expects the sum (22.2) to decay exponentially with n. More precisely, by the hyperbolicity assumption of sect. 18.1.1, the expanding eigenvalue of the Jacobian matrix of the flow is exponentially bounded from both above and below,

$$1 < |\Lambda_{min}| \le |\Lambda(x)| \le |\Lambda_{max}|\,, \tag{22.4}$$

and the area of each strip in (22.2) is bounded by $|\Lambda_{max}^{-n}| \le |\mathcal{M}_i| \le |\Lambda_{min}^{-n}|$. Replacing $|\mathcal{M}_i|$ in (22.2) by its estimates in terms of $|\Lambda_{max}|$ and $|\Lambda_{min}|$ immediately leads to exponential bounds $(2/|\Lambda_{max}|)^n \le \hat{\Gamma}_n \le (2/|\Lambda_{min}|)^n$, i.e.,

$$\ln|\Lambda_{max}| - \ln 2 \ge -\frac{1}{n}\ln\hat{\Gamma}_n \ge \ln|\Lambda_{min}| - \ln 2\,. \tag{22.5}$$

The argument based on (22.5) establishes only that the sequence $\gamma_n = -\frac{1}{n}\ln\Gamma_n$ has a lower and an upper bound for any n. In order to prove that γ_n converge to the limit γ, we first show that for hyperbolic systems the sum over surviving intervals (22.2) can be replaced by a sum over periodic orbit stabilities. By (22.4) the size of the strip $\mathcal{M}_i$ can be bounded by the stability Λ_i of the ith periodic point:

$$C_1\frac{1}{|\Lambda_i|} < \frac{|\mathcal{M}_i|}{|\mathcal{M}|} < C_2\frac{1}{|\Lambda_i|}\,, \tag{22.6}$$

for any periodic point i of period n, with constants C_j dependent on the dynamical system but independent of n. The meaning of these bounds is that for increasingly long cycles in a system of bounded hyperbolicity, the shrinking of the ith strip is better approximated by the derivatives evaluated on the periodic point within the strip. Hence, the survival probability can be bounded close to the periodic point stability sum

$$\hat{C}_1\,\Gamma_n < \sum_i^{(n)}\frac{|\mathcal{M}_i|}{|\mathcal{M}|} < \hat{C}_2\,\Gamma_n\ , \tag{22.7}$$

where $\Gamma_n = \sum_i^{(n)} 1/|\Lambda_i|$ is the asymptotic trace sum (18.26). This establishes that for hyperbolic systems the survival probability sum (22.2) can be replaced by the periodic orbit sum (18.26). exercise 22.1 exercise 16.4

We conclude that for hyperbolic, locally unstable flows the fraction (22.1) of initial x whose trajectories remain trapped within $\mathcal{M}$ up to time t is expected to decay exponentially,

$$\Gamma_{\mathcal{M}}(t) \propto e^{-\gamma t}\,,$$

where γ is the asymptotic *escape rate* defined by

$$\gamma = -\lim_{t\to\infty}\frac{1}{t}\ln\Gamma_{\mathcal{M}}(t)\,. \tag{22.8}$$

22.2 Natural measure in terms of periodic orbits

Let us now refine the reasoning of sect. 22.1 and argue that the trace is a discretized integral over state space. Consider the trace (18.7) in the large time limit (18.25):

$$\mathrm{tr}\,\mathcal{L}^n = \int dx\,\delta(x - f^n(x))\,e^{\beta A^n(x)} \approx \sum_i^{(n)}\frac{e^{\beta A^n(x_i)}}{|\Lambda_i|}\,.$$

The factor $1/|\Lambda_i|$ was interpreted in (22.2) as the area of the ith phase-space strip. Hence, the $\mathrm{tr}\,\mathcal{L}^n$ represents a discrete version of $\int dx\,e^{\beta A^n(x)}$ approximated by a tessellation into strips centered on periodic points x_i, (see figure 1.11), with the volume of the ith neighborhood given by estimate $|\mathcal{M}_i| \sim 1/|\Lambda_i|$, and $e^{\beta A^n(x)}$ estimated by $e^{\beta A^n(x_i)}$, its value at the ith periodic point. If the symbolic dynamics is complete, any state space rectangle $[s_{-m}\cdots s_0.s_1 s_2\cdots s_n]$ always contains the periodic point $\overline{s_{-m}\cdots s_0 s_1 s_2\cdots s_n}$; hence, although the periodic points are of measure zero (just like rationals in the unit interval), they are dense on the non–wandering set. Equipped with a measure for the associated rectangles, periodic orbits suffice to cover the entire non–wandering set. The average of $e^{\beta A^n}$ evaluated on the non–wandering set is therefore given by the trace, properly normalized so that $\langle 1\rangle = 1$: section 12.3.1

$$\left\langle e^{\beta A^n}\right\rangle_n \approx \frac{\sum_i^{(n)} e^{\beta A^n(x_i)}/|\Lambda_i|}{\sum_i^{(n)} 1/|\Lambda_i|} = \sum_i^{(n)}\mu_i\,e^{\beta A^n(x_i)}\,. \tag{22.9}$$

Here μ_i is the *normalized natural measure* section 17.3

$$\sum_i^{(n)}\mu_i = 1\,, \qquad \mu_i = e^{n\gamma_n}/|\Lambda_i|\,, \tag{22.10}$$

which is correct both for closed systems as well as open systems.

Unlike brute numerical slicing of the integration space into an arbitrary lattice (for a critique, see sect. 16.3), periodic orbit theory is smart, as it automatically partitions integrals according to the intrinsic topology of the flow, and assigns to each tile i the invariant natural measure μ_i.

22.2.1 Unstable periodic orbits are dense

(L. Rondoni and P. Cvitanović)

Our goal in sect. 17.1 was to evaluate the space and time averaged expectation value (17.9). An average over all periodic orbits can accomplish the job only if the periodic orbits fully explore the asymptotically accessible state space.

Why should unstable periodic points end up being dense? The cycles are intuitively expected to be *dense* because on a connected chaotic set a typical trajectory is expected to behave ergodically, and infinitely many times pass arbitrarily close to any point on the set (including the initial point of the trajectory itself). The argument proceeds more or less as follows. Partition $\mathcal{M}$ in arbitrarily small regions and consider particles that start in the region $\mathcal{M}_i$, and return to it in n steps after some peregrination in the state space. For example, a trajectory might return a little to the left of its original position, whereas a nearby neighbor might return a little to the right of its original position. By assumption, the flow is continuous, so generically one expects to be able to gently move the initial point in such a way that the trajectory returns precisely to the initial point, i.e., one expects a periodic point of period n in cell i. As we diminish the size of regions $\mathcal{M}_i$, aiming a trajectory that returns to $\mathcal{M}_i$ becomes increasingly difficult. Therefore, we are guaranteed that unstable orbits of increasingly large periods are densely interspersed in the asymptotic non–wandering set.

The above argument is heuristic, by no means guaranteed to work, and it must be checked for the particular system at hand. A variety of ergodic but insufficiently mixing counter-examples can be constructed - the most familiar being a quasiperiodic motion on a torus.

22.3 Correlation functions

The *time correlation function* $C_{AB}(t)$ of two observables A and B along the trajectory $x(t) = f^t(x_0)$ is defined as

$$C_{AB}(t;x_0) = \lim_{T\to\infty}\frac{1}{T}\int_0^T d\tau A(x(\tau+t))B(x(\tau))\,, \qquad x_0 = x(0)\,. \quad (22.11)$$

If the system is ergodic, with invariant continuous measure $\rho_0(x)dx$, then correlation functions do not depend on x_0 (apart from a set of zero measure), and may be computed by a state space average as well,

$$C_{AB}(t) = \int_{\mathcal{M}} dx_0\, \rho_0(x_0)A(f^t(x_0))B(x_0)\,. \quad (22.12)$$

For a chaotic system we expect that time evolution will lose the information contained in the initial conditions, so that $C_{AB}(t)$ will approach the *uncorrelated* limit $\langle A\rangle\cdot\langle B\rangle$. As a matter of fact the asymptotic decay of correlation functions

$$\hat{C}_{AB} := C_{AB} - \langle A\rangle\langle B\rangle \quad (22.13)$$

for any pair of observables coincides with the definition of *mixing*, a fundamental property in ergodic theory. We now assume without loss of generality that $\langle B\rangle = 0$.

(Otherwise we may define a new observable by $B(x) - \langle B\rangle$.) Our purpose is now to connect the asymptotic behavior of correlation functions with the spectrum of the Perron-Frobenius operator $\mathcal{L}$. We can write (22.12) as

$$\tilde{C}_{AB}(t) = \int_{\mathcal{M}} dx \int_{\mathcal{M}} dy\, A(y)B(x)\rho_0(x)\delta(y - f^t(x))$$

and recover the evolution operator

$$\tilde{C}_{AB}(t) = \int_{\mathcal{M}} dx \int_{\mathcal{M}} dy\, A(y)\mathcal{L}^t(y,x)B(x)\rho_0(x).$$

Recall sect. 16.1, where we showed that $\rho(x)$ is the eigenvector of $\mathcal{L}$ corresponding to probability conservation:

$$\int_{\mathcal{M}} dy\, \mathcal{L}^t(x,y)\rho(y) = \rho(x)\,.$$

We can expand the x-dependent part of this equation in terms of the eigenbasis of $\mathcal{L}$:

$$B(x)\rho_0(x) = \sum_{\alpha=0}^{\infty} c_\alpha\rho_\alpha(x)\,,$$

where $\rho_0(x)$ is the natural measure. Since the average of the left hand side is zero the coefficient c_0 must vanish. The action of $\mathcal{L}$ can then be written as

$$\tilde{C}_{AB}(t) = \sum_{\alpha\neq 0} e^{-s_\alpha t}c_\alpha \int_{\mathcal{M}} dy\, A(y)\rho_\alpha(y). \quad (22.14)$$

exercise 22.2

We see immediately that if the spectrum has a *gap*, i.e., if the second largest leading eigenvalue is isolated from the largest eigenvalue ($s_0 = 0$) then (22.14) implies *exponential* decay of correlations

$$\tilde{C}_{AB}(t) \sim e^{-\nu t}\,.$$

The correlation decay rate $\nu = s_1$ then depends only on intrinsic properties of the dynamical system (the position of the next-to-leading eigenvalue of the Perron-Frobenius operator), and the choice of a particular observable influences only the prefactor.

Correlation functions are often accessible from time series measurable in laboratory experiments and numerical simulations; moreover, they are intimately linked to transport exponents.

22.4 Trace formulas *vs.* level sums

> Benoit B. Mandelbrot: "I would be perfectly happy being Kepler" [to a coming fractals' Newton]. Referring to the broad array of things now described by fractals, he added, "I have been Kepler many times over."
>
> —J. Gleick, New York Times, January 22, 1985

Trace formulas (18.10) and (18.23) diverge precisely where one would like to use them, at s equal to eigenvalues s_α. To avoid this divergence, one can proceed as follows; according to (18.27) the "level" sums (all symbol strings of length n) behave asymptotically dominated by the leading eigenvalue $e^{s_0 n}$ of the evolution operator

$$\sum_{i\in \mathrm{Fix} f^n} \frac{e^{\beta A^n(x_i)}}{|\Lambda_i|} \to e^{s_0 n}\,,$$

so an nth order estimate $s_{(n)}$ of the leading eigenvalue s_0 is fixed by the condition

$$1 = \sum_{i\in \mathrm{Fix} f^n} \frac{e^{\beta A^n(x_i)} e^{-s_{(n)} n}}{|\Lambda_i|}\,. \tag{22.15}$$

The eigenvalue condition for the level sum (22.15) can be written in the same form as the two conditions (20.18) and (20.19) given so far:

$$0 = 1 - \sum_i^{(n)} t_i\,, \qquad t_i = t_i(\beta, s(\beta))\,, \qquad n_i = n\,. \tag{22.16}$$

We do not recommended it as a computational method. The difficulty in estimating the leading eigenvalue s_0 from this $n\to\infty$ limit is at least twofold:

1. Due to an exponential growth in the number of intervals and an exponential decrease in the attainable accuracy, the maximum n, achieved experimentally or numerically, is approximately between 5 and 20.

2. The pre-asymptotic sequence of finite estimates $s_{(n)}$ is not unique, because the sums Γ_n depend on how we define the escape region, and because in general the areas $|\mathcal{M}_i|$ in the sum (22.2) should be weighted by the density of initial conditions $\rho(0)$. For example, an overall measuring unit rescaling $|\mathcal{M}_i| \to \alpha|\mathcal{M}_i|$ introduces $1/n$ corrections in $s_{(n)}$ defined by the log of the sum (22.8): $s_{(n)} \to s_{(n)} + \ln\alpha/n$. This problem can be ameliorated by defining a level average

$$\left\langle e^{\beta A(s)}\right\rangle_{(n)} := \sum_{i\in \mathrm{Fix} f^n} \frac{e^{\beta A^n(x_i)} e^{sn}}{|\Lambda_i|} \tag{22.17}$$

and requiring that the ratios of successive levels satisfy

$$1 = \frac{\left\langle e^{\beta A(s_{(n)})}\right\rangle_{(n+1)}}{\left\langle e^{\beta A(s_{(n)})}\right\rangle_{(n)}}\,.$$

This avoids the worst problem with formula (22.15), the inevitable $1/n$ corrections due to its lack of rescaling invariance. However, even though much published pondering of "chaos" relies on it, there is no need for such gymnastics: dynamical zeta functions and spectral determinants are already invariant not only under linear rescalings, but under *all* smooth nonlinear conjugacies $x \to h(x)$, and require no $n\to\infty$ extrapolations to asymptotic times. Comparing this with cycle expansions (20.7), we see the difference; in the level sum approach, we keep increasing exponentially the number of terms with no reference to the fact that most are already known from shorter estimates, but in cycle expansions short terms dominate and longer ones enter only as exponentially small corrections.

22.4.1 Flow conservation sum rules

The trace formula version of the flow conservation sum rule (20.17) comes in two varieties (one for maps and another for flows). By flow conservation, the leading eigenvalue is $s_0 = 0$, which for maps (22.16) yields

$$\mathrm{tr}\,\mathcal{L}^n = \sum_{i\in \mathrm{Fix} f^n} \frac{1}{|\det\,(\mathbf{1} - M^n(x_i))\,|} = 1 + e^{s_1 n} + \dots\,. \tag{22.18}$$

For flows, one can apply this rule by grouping together cycles from $t = T$ to $t = T + \Delta T$

$$\frac{1}{\Delta T}\sum_{p,r}^{T\le rT_p\le T+\Delta T} \frac{T_p}{\left|\det\left(\mathbf{1} - M_p^r\right)\right|} = \frac{1}{\Delta T}\int_T^{T+\Delta T} dt\left(1 + e^{s_1 t} + \dots\right)$$
$$= 1 + \frac{1}{\Delta T}\sum_{\alpha=1}^{\infty} \frac{e^{s_\alpha T}}{s_\alpha}\left(e^{s_\alpha \Delta T} - 1\right) \approx 1 + e^{s_1 T} + \cdots\,. \tag{22.19}$$

As is usual for fixed level trace sums, the convergence of (22.18) is controlled by the gap between the leading and next-to-leading eigenvalues of the evolution operator.

Résumé

We conclude this chapter by a general comment on the relation of finite trace sums such as (22.2) to spectral determinants and dynamical zeta functions. One

might be tempted to believe that given a deterministic rule, a sum like (22.2) can be evaluated to any desired precision. For short times, this is indeed true: every region $\mathcal{M}_i$ in (22.2) can be accurately delineated, and there is no need for any fancy theory. However, if the dynamics is unstable, local variations in initial conditions grow exponentially and in finite time attain the size of the system. The difficulty with estimating the $n \to \infty$ limit from (22.2) is then at least twofold:

1. Due to the exponential growth in number of intervals, and the exponential decrease in attainable accuracy, the maximal n attainable experimentally or numerically is in practice of order of something between 5 to 20;

2. The pre-asymptotic sequence of finite estimates γ_n is not unique, because the sums $\hat{\Gamma}_n$ depend on how we define the escape region, and because in general the areas $|\mathcal{M}_i|$ in the sum (22.2) should be weighted by the density of initial x_0.

In contrast, dynamical zeta functions and spectral determinants are invariant under *all* smooth nonlinear conjugacies $x \to h(x)$, not only linear rescalings, and require no $n \to \infty$ extrapolations.

Commentary

Remark 22.1 Nonhyperbolic measures. The measure $\mu_i = 1/|\Lambda_i|$ is the natural measure only for the strictly hyperbolic systems. For non-hyperbolic systems, the measure might develop cusps. For example, for Ulam maps (unimodal maps with quadratic critical point mapped onto the "left" unstable fixed point x_0, discussed in more detail in chapter 24), the measure develops a square-root singularity on the $\overline{0}$ cycle:

$$\mu_0 = \frac{1}{|\Lambda_0|^{1/2}} \,. \tag{22.20}$$

Thermodynamic averages are still expected to converge in the "hyperbolic" phase in which the positive entropy of unstable orbits dominates the marginal orbits, but they fail in the "non-hyperbolic" phase. The general case remains unclear [12.12, 22.2, 22.3, 22.4, 22.6].

Remark 22.2 Trace formula periodic orbit averaging. The cycle averaging formulas are not the first thing one intuitively writes down; the approximate trace formulas are more accessibly heuristically. Trace formula for averaging (22.19) seems to have been discussed for the first time by Hannay and Ozorio de Almeida [22.9, 6.9]. Another novelty of cycle averaging formulas is one of their main virtues, in contrast to the explicit analytical results such as those of ref. [20.4]. Their evaluation *does not* require any explicit construction of the (coordinate dependent) eigenfunctions of the Perron-Frobenius operator (i.e., the natural measure ρ_0).

Remark 22.3 Role of noise in dynamical systems. In any physical application, the dynamics is always accompanied by external noise in addition to deterministic chaos.

The former can be characterized by its strength σ and distribution. Lyapunov exponents, correlation decay, and dynamo rate can be defined in this case the same way as in the deterministic case. One might think that noise completely destroys the results derived here. However, as we show chapter 28, deterministic formulas remain valid to accuracy comparable with noise width if the noise level is small. A small level of noise even helps, as it makes the dynamics more ergodic. Deterministically non-communicating parts of state space become weakly connected due to noise. This argument explains why periodic orbit theory is also applicable to non-ergodic systems. For small amplitude noise, one can expand perturbatively

$$\overline{a} = \overline{a}_0 + \overline{a_1}\sigma^2 + \overline{a_2}\sigma^4 + \dots \,,$$

around the deterministic averages a_0. The expansion coefficients $\overline{a_1}, \overline{a_2}, \dots$ can also be expressed in terms of periodic orbit formulas. Calculating these coefficients is one of the challenges facing periodic orbit theory, discussed in refs. [16.9, 16.10, 16.11].

Exercises

22.1. **Escape rate of the logistic map.**

(a) Calculate the fraction of trajectories remaining trapped in the interval $[0, 1]$ for the logistic map

$$f(x) = A(1 - (2x - 1)^2), \tag{22.21}$$

and determine the A dependence of the escape rate $\gamma(A)$ numerically.

(b) Develop a numerical method for calculating the lengths of intervals of trajectories remaining stuck for n iterations of the map.

(c) Describe the dependence of A near the critical value $A_c = 1$?

22.2. **Four-scale map correlation decay rate.** Consider the piecewise-linear map

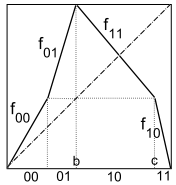

$$f(x) = \begin{cases} f_{00} = \Lambda_0 x \\ f_{01} = s_{01}(x - b) + 1 \\ f_{11} = \Lambda_1(x - b) + 1 \\ f_{10} = s_{10}(x - 1) \end{cases}$$

with a 4-interval state space Markov partition

$$\begin{aligned} \mathcal{M} &= \{\mathcal{M}_{00}, \mathcal{M}_{01}, \mathcal{M}_{10}, \mathcal{M}_{11}\} \\ &= \{[0, b/\Lambda_0], (b/\Lambda_0, b](b, c](c, 1]\} \,. \end{aligned}$$

(a) compute s_{01}, s_{10}, c.

(b) Show that the 2-cycle Floquet multiplier does not depend on b,

$$\Lambda_{01} = s_{01}s_{10} = -\frac{\Lambda_0\Lambda_1}{(\Lambda_0 - 1)(\Lambda_1 + 1)} \,.$$

(c) Write down the $[2\times2]$ Perron-Frobenius operator acting on the space of densities piecewise constant over the four partitions.

(d) Construct the corresponding transition graph.

(e) Write down the corresponding spectral determinant.

(f) Show that the escape rate vanishes, $\gamma = -\ln(z_0) = 0$.

(g) Determine the spectrum of the Perron-Frobenius operator on the space of densities piecewise constant over the four partitions. Show that the second largest eigenvalue of the is $\frac{1}{z_1} = -1 + \frac{1}{\Lambda_0} - \frac{1}{\Lambda_1}$.

(h) Is this value consistent with the tent map value previously computed in exercise 16.4 (with the appropriate choice of $\{\Lambda_0, \Lambda_1, c\}$).

(i) (optional) Is this next-to leading eigenvalue still correct if the Perron-Frobenius operator acts on the space of analytic functions?

22.3. **Lyapunov exponents for 1-dimensional maps.** Extend your cycle expansion programs so that the first and the second moments of observables can be computed. Use it to compute the Lyapunov exponent for the following maps:

(a) the piecewise-linear skew tent (flow conserving map)

$$f(x) = \begin{cases} \Lambda_0 x & \text{if } 0 \le x < \Lambda_0^{-1}, \\ \Lambda_1(1-x) & \text{if } \Lambda_0^{-1} \le x \le 1. \end{cases} ,$$

$\Lambda_1 = \Lambda_0/(\Lambda_0 - 1)$.

(b) the Ulam map $f(x) = 4x(1-x)$.

(c) the skew Ulam map

$$f(x) = \Lambda_0 x(1-x)(1-bx), \qquad (22.22)$$

$1/\Lambda_0 = x_c(1-x_c)(1-bx_c)$. In our numerical work we fix (arbitrarily, the value chosen in ref. [20.3]) $b = 0.6$, so

$$f(x) = 0.1218\, x(1-x)(1-0.6\,x)$$

with a peak $f(x_c) = 1$ at $x_c = 0.7$.

(d) the repeller of $f(x) = Ax(1-x)$, for either $A = 9/2$ or $A = 6$ (this is a continuation of exercise 20.2).

(e) the 2-branch flow conserving map

$$\begin{aligned} f_0(x) &= \frac{1}{2h}\left(h - p + \sqrt{(h-p)^2 + 4hx}\right) \\ f_1(x) &= \frac{1}{2h}(h + p - 1) \qquad (22.23) \\ &\quad + \frac{1}{2h}\sqrt{(h+p-1)^2 + 4h(x-p)}\,, \end{aligned}$$

with a 2-interval state space Markov partition $\mathcal{M} = \{\mathcal{M}_0, \mathcal{M}_1\} = \{[0,p],(p,1]\}$. This is a nonlinear perturbation of the Bernoulli shift map, for which $h = 0$ (23.6); the first 15 eigenvalues of the Perron-Frobenius operator are listed in ref. [22.1] for $p = 0.8$, $h = 0.1$. Use these parameter values when computing the Lyapunov exponent.

Cases (a) and (b) can be computed analytically; cases (c), (d) and (e) require numerical computation of cycle stabilities. Just to see whether the theory is worth the trouble, also check your cycle expansions results for cases (c) and (d) with Lyapunov exponents computed by direct numerical averaging along trajectories of randomly chosen initial points:

(f) trajectory-trajectory separation (17.32) (hint: rescale δx every so often, to avoid numerical overflows),

(g) iterated stability (17.37).

How good is the numerical accuracy compared with periodic orbit theory predictions for (a) - (g)?

References

[22.1] F. Christiansen, G. Paladin and H.H. Rugh, *Phys. Rev. Lett.* **65**, 2087 (1990).

[22.2] A. Politi, R. Badii and P. Grassberger, *J. Phys. A* **15**, L763 (1988).

[22.3] P. Grassberger, R. Badii and A. Politi, "Scaling laws for invariant measures on hyperbolic and nonhyperbolic attractors," *J. Stat. Phys.* **51**, 135 (1988).

[22.4] E. Ott, C. Grebogi and J.A. Yorke, *Phys. Lett. A* **135**, 343 (1989).

[22.5] C. Grebogi, E. Ott and J.A. Yorke, *Phys. Rev.* **A 36**, 3522 (1987).

[22.6] C. Grebogi, E. Ott and J. Yorke, *Physica* **D 7**, 181 (1983).

[22.7] C. Grebogi, E. Ott and J.A. Yorke, *Phys. Rev.* **A36**, 3522 (1987).

[22.8] C. Grebogi, E. Ott and J. Yorke, "Unstable periodic orbits and the dimension of multifractal chaotic attractors," *Phys. Rev. A* **37**, 1711 (1988).

[22.9] J. H. Hannay and A. M. Ozorio de Almeida, *J. Phys.* **A 17**, 3429, (1984).

[22.10] L. Kadanoff and C. Tang, *Escape from strange repellers*, *Proc. Natl. Acad. Sci. USA*, **81**, 1276 (1984).

[22.11] T. Tél, "On the organization of transient chaos: Application to irregular scattering," in Bai-lin Hao, ed., *Directions in Chaos*, vol. 3, (World Scientific, Singapore 1988) p. 149,

[22.12] T. Tél, *J. Phys.* **A22**, L691 (1989).

[22.13] S. Bleher, C. Grebogi and J.A. Yorke, *Physica* **46D**, 87 (1990),

[22.14] D. Ruelle, *J. Stat. Phys.* **44**, 281 (1986).

[22.15] W. Parry and M. Pollicott, *Ann. Math.* **118**, 573 (1983).

[22.16] P. Cvitanović, "Invariant measurements of strange sets in terms of cycles," *Phys. Rev. Lett.* **61**, 2729 (1988).

[22.17] E.G. Altmann and T. Tél, "Poincare recurrences and transient chaos in leaked systems," (2008); `arXiv:0808.3785`.